# Lab on a Chip

Micro- & nano- fluidic research for chemistry, physics, biology, & bioengineering

www.rsc.org/loc

Volume 11 | Number 10 | 21 May 2011 | Pages 1701–1840

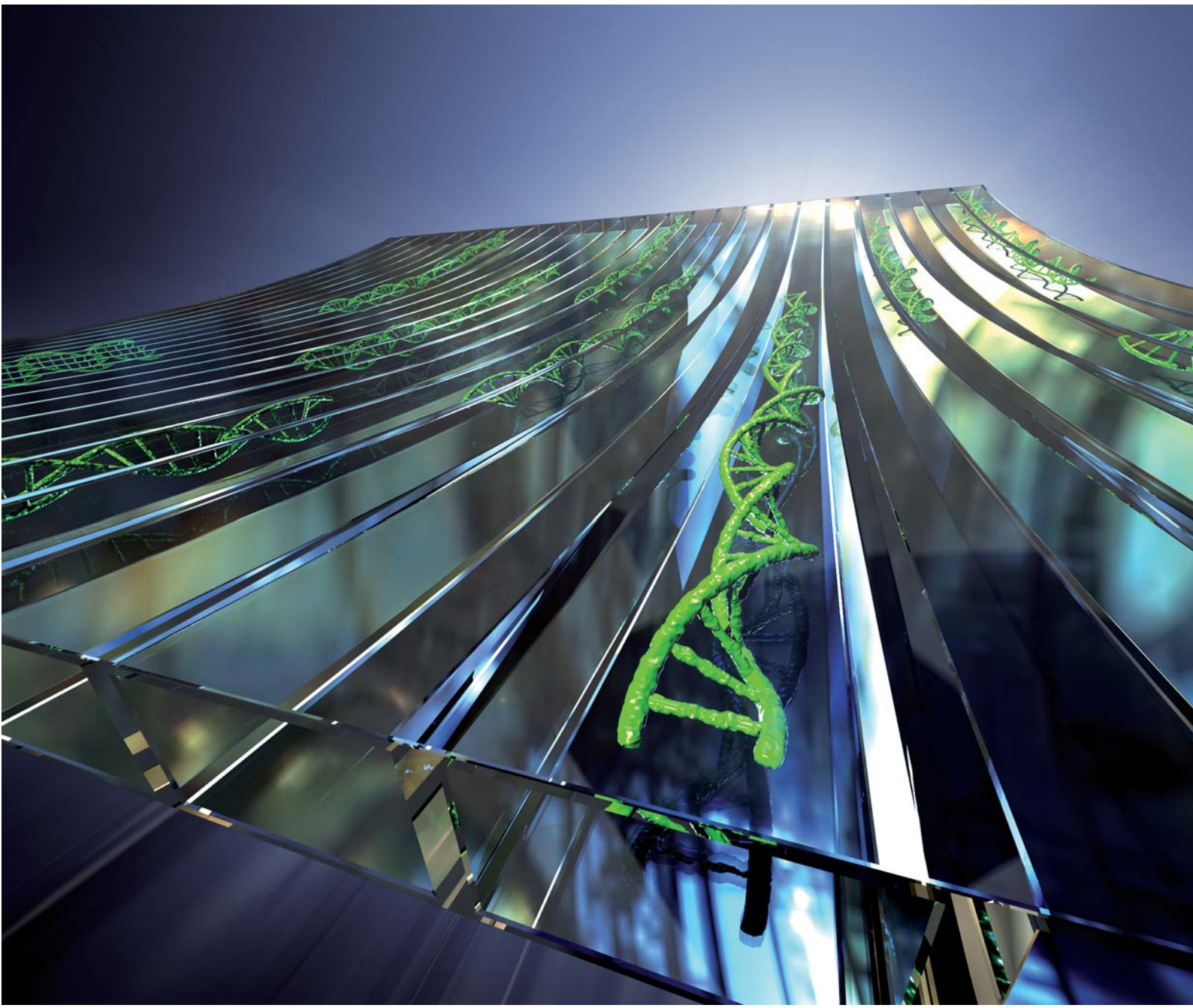

ISSN 1473-0197

RSC Publishing

**PAPER**

*Jo et al.*

Nanochannel confinement: DNA stretch approaching full contour length

1473-0197(2011)11:10;1-6

Lab on a Chip

Dynamic Article Links

Cite this: *Lab Chip*, 2011, **11**, 1721

www.rsc.org/loc

**PAPER**



# Nanochannel confinement: DNA stretch approaching full contour length

**Yoori Kim,[a] Ki Seok Kim,[b] Kristy L. Kounovsky,[c] Rakwoo Chang,[d] Gun Young Jung,[b] Juan J. dePablo,[e] Kyubong Jo*[a] and David C. Schwartz*[c]**

***Received 10th December 2010, Accepted 25th February 2011***
**DOI: 10.1039/c0lc00680g**

Fully stretched DNA molecules are becoming a fundamental component of new systems for comprehensive genome analysis. Among a number of approaches for elongating DNA molecules, nanofluidic molecular confinement has received enormous attentions from physical and biological communities for the last several years. Here we demonstrate a well-optimized condition that a DNA molecule can stretch almost to its full contour length: the average stretch is 19.1 μm ± 1.1 μm for YOYO-1 stained λ DNA (21.8 μm contour length) in 250 nm × 400 nm channel, which is the longest stretch value ever reported in any nanochannels or nanoslits. In addition, based on Odijk's polymer physics theory, we interpret our experimental findings as a function of channel dimensions and ionic strengths. Furthermore, we develop a Monte Carlo simulation approach using a primitive model for the rigorous understanding of DNA confinement effects. Collectively, we present a more complete understanding of nanochannel confined DNA stretching *via* the comparisons to computer simulation results and Odijk's polymer physics theory.

## Introduction

Many of the recent advances in the genomic sciences are directly linked with new molecular insights and tools that manipulate and analyze DNA molecules in new ways.[1,2] This is evidenced by the explosion of new platforms for DNA sequencing,[3,4] analyzing molecular libraries comprising single DNA molecules, which are promising the commoditization of sequence information.[5] Even newer sequencing approaches are leveraging the direct analysis of individual DNA molecules for engendering "third generation sequencing".[6–9] A critical advantage of sequencing systems using single molecule analytes is that they obviate the need for template amplification, a feature that not only saves time and reduces reagent costs but more importantly points the way for the development of new approaches offering significantly longer read lengths. Such advantages potentiate comprehensive genome analysis that elucidates all parts of a genome for careful analysis. Unfortunately, most contemporary single DNA molecule sequencing approaches are limited to the analysis of short DNA fragments usually with less than hundreds of base pairs.[1]

On the other hand, stretched genomic DNA molecules from tens of kilobases to megabases (μm to mm in length) are promising analytes because they intrinsically reveal the location of each sequence read along the same, long DNA molecule.[9–12] These advantages for mapping, though not sequencing, entire genomes were originally pioneered through development of the optical mapping system.[13–17] Briefly, optical mapping generated physical genomic maps have been utilized for guiding sequence assembly for numerous genome projects,[18] and detecting large scale genomic variations,[19,20] and DNA methylation.[21] In addition to physical genomic maps, elongated DNA molecules on the surface have also been utilized as platforms for biochemical studies such as RNA polymerase on DNA backbones,[22] and also extended to a novel sequencing technology like optical sequencing.[9] Even though elongated DNA molecules deposited on the surface have been versatile analytes for many different biochemical applications, they have intrinsic limitations due to the surface fixation and difficulties in controlling surface properties. In order to overcome these limitations caused by DNA fixation on the surface, we have recently developed nano-/microfluidic approaches for dynamic elongation of single DNA molecules.[10,23] Over the surface fixation, these fluidic components for DNA elongation offer the advantage of facile integration into more sophisticated microfluidic devices as a micro-total analytical system (μTAS).

Nanochannel confined DNA elongation is now being actively investigated to the direction of high-throughput DNA analysis with high resolution.[10,24–26] Toward high resolution DNA

[a]*Department of Chemistry and Interdisciplinary Program of Integrated Biotechnology, Sogang University, Seoul, 121-742, Republic of Korea. E-mail: jokyubong@sogang.ac.kr; Tel: +82 2 705 8881*
[b]*School of Material Science and Engineering, Gwangju Institute of Science and Technology (GIST), Gwangju, 500-712, Republic of Korea*
[c]*Laboratory for Molecular and Computational Genomics, Department of Chemistry, Laboratory of Genetics, University of Wisconsin–Madison, Madison, Wisconsin, 53706, USA. E-mail: dcschwartz@wisc.edu; Tel: +1 608 265-0546*
[d]*Department of Chemistry, Kwangwoon University, Seoul, 139-701, Republic of Korea*
[e]*Department of Chemical and Biological Engineering, University of Wisconsin–Madison, 1415 Engineering Drive, Madison, WI, 53706, USA*

analysis, the first goal of DNA elongation in nanochannels is to attain fully stretched DNA molecules without knots or hairpins. Simultaneously, to achieve a high-throughput analytical system, nanochannels should be large enough for efficient DNA loading using a conventional nanofabrication technology instead of superb nanotechnology difficult to follow. In addition, for practical biological applications, disposable and flexible polydimethylsiloxane (PDMS) material is more promising than any other solid materials.[27] Accordingly, here we have pursued to design an optimum system for long stretch of DNA molecules in reasonable nanochannel dimensions by using practical materials.

For a system design, it is naturally expected that DNA elongation can be accomplished by reducing dimensions of nanoconfinement.[28] Nanochannels would be ideal if they are slightly larger than the diameter of double helical DNA molecules, which would result in the stretching up to their full contour length. However, there are limitations in reducing channel dimensions: first, the fabrication of very small nanochannels with long length is extremely challenging.[29] In general, smaller nanochannels require more advanced and more expensive nanofabrication technologies. Second, the DNA loading efficiency into very small nanochannels is dramatically reduced.[30] As an alternative way of reducing the channel dimension, the DNA stretch can be enhanced by increasing the persistence length of DNA or by increasing polymer's stiffness, which was previously demonstrated by lowering ionic strengths.[10] However, the optimum condition for channel dimension and ionic strength has yet to be found. Accordingly, our overarching goal in this study here is to achieve fully stretched DNA molecules by adjusting channel dimensions and ionic strengths with the aid of theory and computer simulation.

## Results

### DNA stretching mediated by nanoconfinement geometry and ionic strength

Our scheme for increasing the DNA stretch was to both minimize nanochannel dimensions using PDMS replica molding techniques and buffer ionic strength conditions. We first fabricated a series of PDMS nanoslit devices using interference lithography and replica molding with the following dimensions (nm; width × height): 250 × 100, 250 × 150, 250 × 250, 400 × 250, 600 × 250, 800 × 250, and 900 × 250; the length of each channel is about 140 μm. Among them, the 250 nm × 250 nm (Fig. 1A) is the smallest dimension of nanochannels into which we have successfully and reproducibly loaded λ DNA molecules (see Experimental).

Very low ionic strength conditions were established by careful illumination conditions instead of using anti-photobleaching agents which increase the ionic strength. In our previous report,[10] we boosted the DNA stretch ($X/L$) to 0.60 ($X$ is defined as the average apparent length and $L$ is the dye adjusted polymer contour length, $L$, 21.8 μm for λ DNA; a stretch of 1.0 indicates complete elongation) in nanoslits (1000 nm × 100 nm) by decreasing the ionic strength of loading buffer. However, there were limitations of stretching because we did not use high resolution lithography technology. In addition, we also found that we could not further increase DNA stretching because β-mercaptoethanol, an anti-photobleaching agent, affects the ionic strength *via* protonic dissociation from a thiol group ($pK_a$ of 9.6).[31] Unfortunately, anti-bleaching agents are an essential part of fluorescence imaging for preventing photobleaching and photolysis, but generally, they perturb the ionic strength: *e.g.*, dithiothreitol (DTT; $pK_a = 9.2$), ascorbic acid (vitamin C; $pK_a = 4.2$), and the oxygen scavenger system using glucose oxidase and catalase.[31] Accordingly, we developed an imaging approach obviating the need for anti-photobleaching agents through judicious illumination conditions (see Experimental).

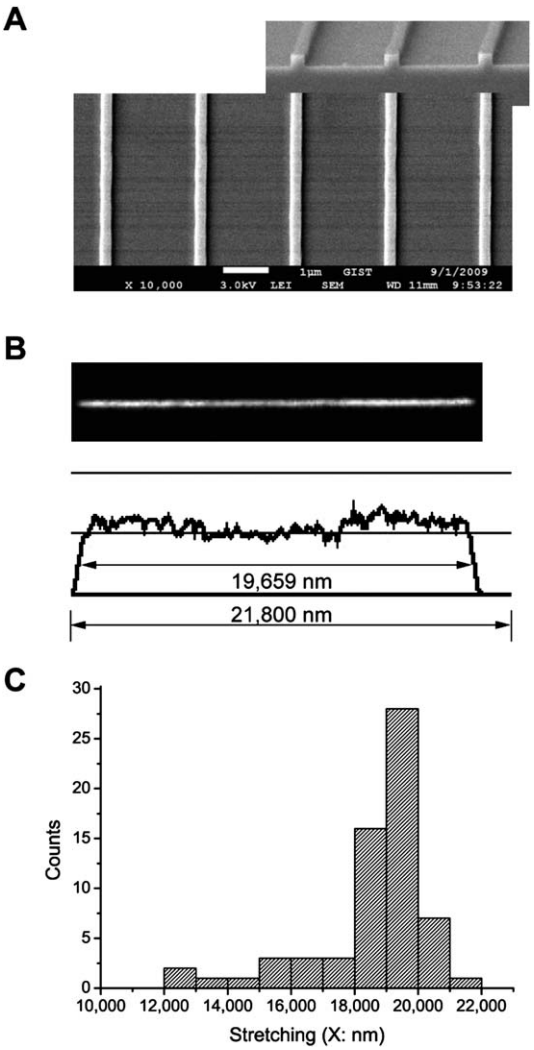


**Fig. 1** (A) Scanning electron micrograph of 250 nm × 250 nm channel's template on a silicon wafer fabricated by interference lithography. The nanochannel template is utilized for replica molding of PDMS nanochannels into which DNA molecules are loaded. (B) Fluorescence micrograph and fluorescence intensity profile of an individual λ DNA molecule (48.5 kb, contour length is 21.8 μm; YOYO-1 stained) in a nanochannel (250 nm × 250 nm). The molecular length is 19.7 μm, which is 90% of its contour length of 21.8 μm. (C) Histogram of DNA stretches in 250 nm × 250 nm channels. The average length is 18.7 μm ± 1.9 μm but the most abundant range is 19 μm to 20 μm.

Fig. 1B presents an image of the λ DNA molecule in 1/40× TE solution (1× TE: 10 mM Tris and 1 mM EDTA titrated with HCl to pH 8.0). The molecule is 19.7 μm long ($X/L = 0.90$ for YOYO-1 stained λ DNA), examined with an intensity profile (Fig. 1B).

The intensity profile analysis not only gives the estimation of molecular length but also allows identifying DNA's conformational details, which facilitates easy differentiation of fully elongated molecules from folded ones. For example, the intensity profile in Fig. 1B depicts a little higher intensity at the ends of molecule, which can be interpreted as the ends of the DNA molecule are more relaxed compared to the well-stretched central portions, which may be due to polymer ends having more entropic freedom than internal segments.[23,32] Using this method, we examined a total 66 stretched λ DNA molecules in the 250 × 250 nm nanochannels as the histogram presented in Fig. 1C. The most abundant range is from 19 μm to 20 μm, whereas the average stretch is 18.7 μm with the standard deviation of 1.9 μm.

For a highly stretched polymer chain, as what we studied here, Odijk developed a model to explain the deflection-dominant polymer elongation in nanochannels using a scaling relationship in 1983,[33] and recently refined his model to an analytical equation as given by[10,34]

$$X/L = 1 - 0.085\left(\left(\frac{A}{P}\right)^{2/3} + \left(\frac{B}{P}\right)^{2/3}\right) \quad (1)$$

where $X$ is the observed elongated length, $L$ is the polymer contour length, $A$ and $B$ are, respectively, channel width and height, and $P$ is the polymer persistence length. The polymer persistence length ($P$) can be calculated from the ionic strength by an equation developed by Odijk,[35] Skolnick and Fixman (OSF).[36] This OSF equation is given by

$$P = P_0 + P_{el} = P_0 + \frac{1}{4\kappa^2 l_B} = P_0 + 0.0324 I^{-1}\ \text{nm} \quad (2)$$

where $P_0$ is the non-electrostatic intrinsic persistence length due to base stacking, $P_{el}$ is the electrostatic persistence length due to intrachain repulsion, $\kappa$ is the inverse of the Debye–Hückel screening length, $l_B$ is the Bjerrum length (0.7 nm in water) and $I$ is the ionic strength of the solution.[37] Odijk's equation (eqn (1)) combined with the OSF equation (eqn (2)) can predict the DNA stretching in nanochannels at a specific ionic strength for various channel dimensions.

Although the OSF equation (eqn (2)) uses a term for ionic strength, to the best of our knowledge, it has never been experimentally validated for multivalent ions. Please note that Skolnick and Fixman, and Bauman *et al.* used only monovalent ions (*e.g.* NaCl) to validate the OSF equation.[36,37] Furthermore, Bauman *et al.* proved that the OSF equation is not applicable to multivalent cations,[37] since multiple charges can collapse DNA structure.[38] Accordingly, we have concluded that it may not be appropriate to use the calculated ionic strength from the buffer components. Instead, we measured the conductivity of diluted TE buffer and compared its conductivity value with equivalent sodium chloride (NaCl) solution. In the case of 1/40× TE, the conductivity corresponds to 0.12 mM NaCl solution, which roughly agrees with the positive Tris ion concentration (0.13 mM) in 1/40× TE solution. Hence, in this paper we use 0.12 mM as the ionic strength for 1/40× TE solution.

Before calculating the persistence length from the ionic strength, we have to determine another term in the OSF equation (eqn (2)), the non-electrostatic intrinsic persistence length ($P_0$). For native DNA, $P_0$ is known to be 50 nm,[37] but there are three different opinions for $P_0$ of DNA stained with bis-intercalator YOYO-1 (*e.g.* 66 nm,[39] 12 nm,[40] and 44 nm[41]). The idea of 66 nm originated from the assumption that $P_0$ may increase in the same ratio as DNA contour length increases.[39] It is well-known that the staining of YOYO-1 increases the contour length of DNA by about 30% because dyes intercalate into stacks of base pairs; for example, native λ DNA has the contour length of 16.5 μm (0.34 nm × 48 502 base pairs), but YOYO-1 intercalated λ DNA has the contour length of 21.8 μm. On the other hand, an optical trapping experiment reported that $P_0$ could be 12 nm,[40] but this value seems too small to explain other experimental observations. Recently, Zhang *et al.* reported that $P_0$ should be 44 nm according to their calculation which takes the effect of positive charges in YOYO-1 molecules into account.[41] They claimed that $P_0$ of 44 nm agreed well with their experimental observations. At the ionic strength of 0.12 mM, the OSF equation predicts the DNA persistence length ($P$) would be 320 nm, 336 nm, 282 nm, and 314 nm for $P_0$ = 50 nm, 66 nm, 12 nm, and 44 nm, respectively. Interestingly, whatever value be used for $P_0$ except 12 nm, the calculated stretch of the λ DNA by Odijk's theory (eqn (1)) is about 18.7 μm ($X/L$ = 0.86), which agrees well with our experimental finding (18.7 μm ± 1.9 μm in the 250 nm × 250 nm nanochannel). Therefore, we use 50 nm as a primary $P_0$, with additional graphs drawn by using 44 nm and 66 nm $P_0$ values (see Figs. 2 and 3).Given a specific ionic strength, we demonstrate that Odijk's equation (eqn (1)) with the OSF equation (eqn (2)) can predict the DNA stretch in a nanochannel with good agreement to experiments. This theory also predicts that the DNA stretch would decrease as the ionic strength increases in a nanochannel, which should be validated by experiments. In our previous report,[10] we controlled the ionic strengths by the degree of dilution of 1× TE, but the multivalent ionic state of EDTA makes the interpretation more complicated as mentioned in the previous paragraph. Hence, here we controlled ionic strengths by adding NaCl (0.2 mM–2.0 mM) into the DNA solution of 1/40× TE. In addition, we did not use anti-bleaching agents to avoid the complication of calculating ionic strengths. As shown in Fig. 2A, we clearly demonstrate that the DNA stretch decreases with the increase of ionic strength as predicted by the Odijk's theory despite the fact that its validity has been disputed.[34,41–43] For this analysis, we used 50 nm as a primary $P_0$, but we also present predictions with different $P_0$ such as 66 nm and 44 nm for comparison. Since all the graphs using three $P_0$ stay in our experimental error ranges, we cannot tell which value of $P_0$ is correct for YOYO-1 stained DNA from these data.

In addition, we compared our experimental results with de Gennes' scaling blob theory: $X/L \approx (wP/D^2)^{1/3}$; $w$: molecular width and $D$: diameter of the channel.[28,44] As shown in the left inset of Fig. 2A, the log–log plot ($X/L$ *vs.* $P$) suggests that three data points of short persistence lengths seem to follow 1/3 scaling relation, but the other four points of long persistence lengths obviously deviate from the scaling relation. For direct comparison, Odijk's equation (eqn (1)) for rectangular channels has been rewritten to a form for square channels like $1 - X/L = 0.085 \times 2(A/P)^{2/3}$.

This rewritten expression is equivalent to Odijk's original scaling relationship:[33,34]

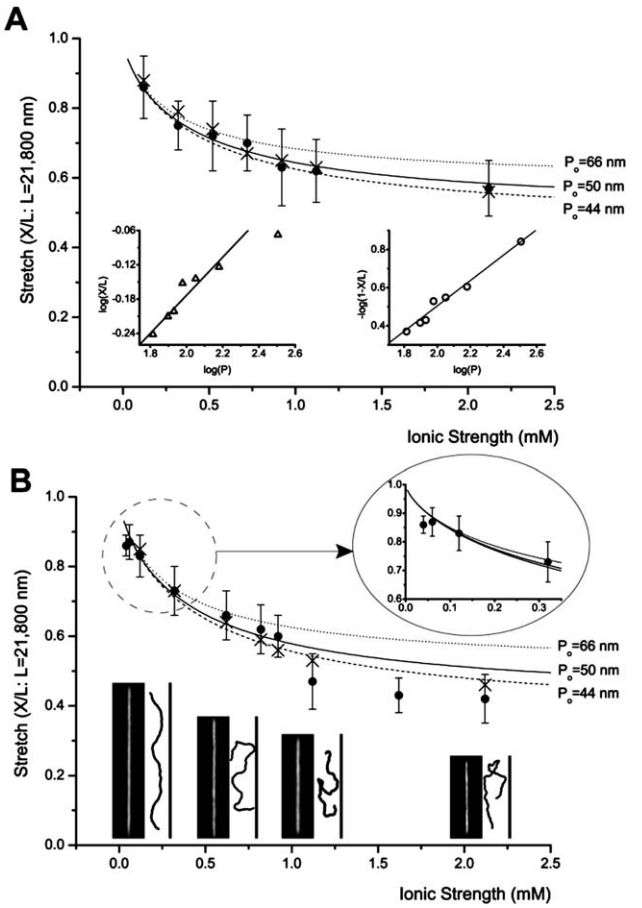


**Fig. 2** Ionic strength dependence of DNA stretching. These graphs include experiment (●: closed circle) and simulation (×: cross) with graphs of Odijk's equation (eqn (1)), in which the persistence length $P$ is determined by OSF equation (eqn (2)). However, this equation is drawn in three different graphs using different non-electrostatic intrinsic persistence length ($P_0$) values such as 50 nm, 66 nm,[39] and 44 nm.[41] Each experimental data point represents measurement from 30 to 200 molecules; error bars show standard deviations of measured lengths. (A) DNA stretching in 250 nm × 250 nm channels: The left inset depicts a log–log plot of de Gennes relationship of $X/L \approx (wP/D^2)^{1/3}$, and the right inset depicts a log–log plot of Odijk's equation for square channels $1 - X/L = 0.085 \times 2(A/P)^{2/3}$. This linear relationship shows $R^2 = 0.98$. (B) DNA stretching in 250 nm × 400 nm channels: magnified plot describes the details of low ionic strengths (1/80× TE and 1/120× TE). Representative fluorescence images of DNA molecules are compared with simulation snapshots at four ionic strengths: 0.12 mM, 0.62 mM, 1.12 mM, and 2.12 mM. Simulation snapshots are magnified for better comparison.

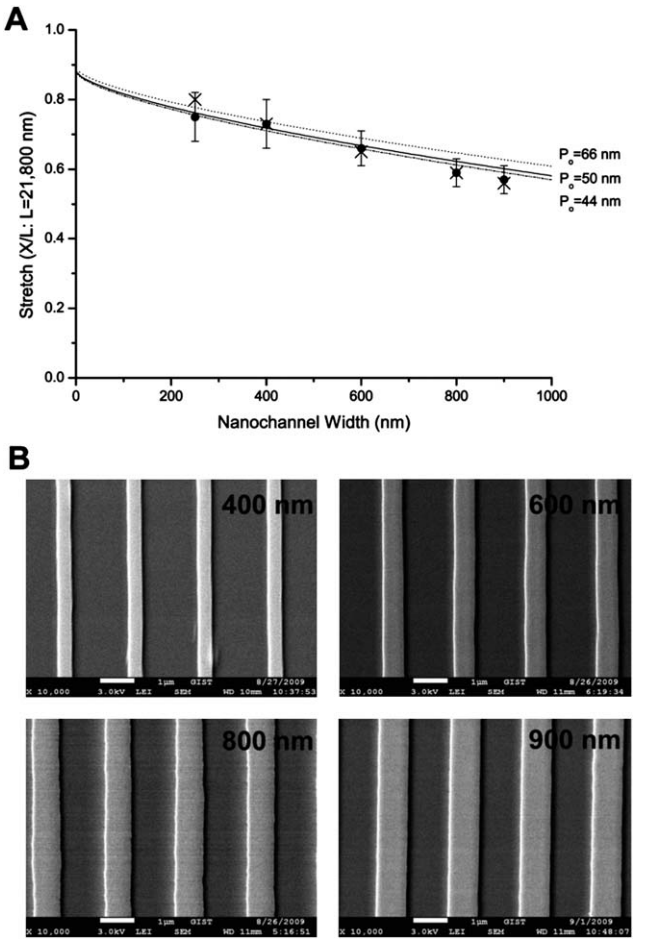


**Fig. 3** Width dependence of DNA stretches with the same height of 250 nm at the fixed ionic strength (1/40× TE and 0.2 mM NaCl). (A) The graph shows experiment (●: closed circle) and simulation (×: cross) with three graphs of Odijk's equation (eqn (1)) using three different non-electrostatic intrinsic persistence length ($P_0$) values such as 50 nm, 66 nm,[39] and 44 nm.[41] Each experimental data point represents measurement from 40 to 90 molecules; error bars show standard deviations of measured lengths. The molecular length is determined by intensity profile analysis illustrated in Fig. 1. We do not include error bars of the simulation result because their standard deviation is very small (≤1%). (B) Scanning electron micrographs of 250 nm × 400, 600, 800, 900 nm channels' template on silicon wafer fabricated by interference lithography. The nanochannel templates were utilized for replica molding of PDMS nanochannels for DNA loading.

$$X/L = \cos\ \theta \cong 1 - \frac{\theta^2}{2} \text{ where } \theta^2 \approx \left(\frac{A}{P}\right)^{2/3} \quad (3)$$

As shown in the right inset of Fig. 2A, the log–log plot ($1 - X/L$ *vs.* $P$) shows better linearity ($R^2 = 0.98$). These analyses indicate that Odijk's analytical equation describes highly stretched DNA molecules in nanochannels in a more appropriate manner than de Gennes scaling relationship.

We extended the theory validation from a square channel (250 nm × 250 nm) to a rectangular channel (250 nm × 400 nm). Interestingly, Odijk's equation (eqn (1)) is only valid below 1 mM, and three points above 1 mM show distinct deviations. Notice that all deviated stretches are less than 50% of its contour length (Fig. 2B). This deviation may suggest the existence of a theoretical regime boundary where polymer's deflection is not dominant anymore.

As opposed to adding more salts, we added more water to dilute 1/40× TE to 1/80× TE (see magnified graph in Fig. 2B). In this condition, we observed that the average stretch of λ DNA is 19.1 μm ± 1.1 μm in 250 nm × 400 nm channels that is the longest average length ever reported in any nanochannels, though it is little lower than Odijk's prediction of 19.3 μm. To get a longer DNA stretch, we attempted loading 1/80× TE DNA solution into 250 nm × 250 nm channels, but we could not succeed in DNA loading. From these results, it seems that DNA

 

elongates more in the condition of 1/80× TE in 250 nm × 400 nm channels compared to 1/40× TE in 250 nm × 250 nm channels shown in Fig. 1. However, histogram analysis reveals that although the dominant peaks are located in the range from 19 μm to 20 μm in both conditions, the number of short stretched molecules is fewer in the condition of 1/80× TE in 250 nm × 400 nm nanochannels (data not shown): *i.e.*, the reduction in number of short stretching molecules is the actual cause of the longest average stretching in 250 nm × 400 nm channels.

To increase the DNA stretch, we dropped the TE concentration to 1/120× TE; we measured the conductivity to confirm its ionic strength. As opposed to our expectation, the average stretch actually decreased to 18.7 μm ± 0.7 μm whereas Odijk's theory predicts 19.9 μm at 1/120× TE in 250 nm × 400 nm channels. In addition, we also attempted more diluted conditions like 1/240× TE and others, but we have not got any success in loading DNA into nanochannels. Now we have not fully understood why stretches do not reach Odijk's prediction at 1/120× TE and why DNA molecules do not enter nanochannels at very low ionic strength conditions. However, we suspect that the deviation of Odijk's prediction and unsuccessful loadings at very low ionic strengths in 250 nm × 400 nm channels may be related to unsuccessful loading of smaller channels previously mentioned in this paper (*e.g.* 250 nm × 100 nm with 1/40× TE). Consequently, these observations imply that more elaborate theoretical models are necessary for the complete understanding.

### Monte Carlo simulation

Computer simulations provide a useful means of investigating the structure of nanochannel-confined DNA at low ionic strengths. Past simulations of confined DNA have been largely focused on high ionic strength systems.[45,46] Some of our observations for low ionic strengths, however, remain to be explained.[41,47] In this work we use Monte Carlo simulations of a "primitive" model of DNA molecule in a nanochannel. In this model, the DNA molecule is represented as a linear chain of $N$ charged spherical monomers, with diameter $\sigma$ and charge $-Ze$ ($Z$ and $e$ are the charge valence and the elementary charge). The rectangular nanochannel is represented by hard walls having the same dimensions as those employed in our experiments. In this study $N$ and $\sigma$ are set to 256 and 10 nm, respectively. The contour length of our model DNA is approximately 2.56 μm, consistent with our experiments. The monomer charge valence $Z$ is set to 20 because it is known that the bare charge density of YOYO-1 stained DNA is around $-2$ $e$/nm.[41]

The interaction between monomers is the sum of hard-sphere ($U_{hs}$) and electrostatic ($U_{elec}$) interactions, which are respectively defined as

$$U_{hs}(r) = \begin{cases} \infty & \text{if } r \le \sigma \\ 0 & \text{otherwise} \end{cases} \quad \text{and} \quad \frac{U_{elec}(r)}{k_B T} = \frac{l_B Z^2 \exp(-\kappa r)}{r} \qquad (4)$$

where $k_B$, $T$, $l_B$, and $\kappa$ are, respectively, the Boltzmann constant, the absolute temperature, the Bjerrum length and the inverse of the Debye length. The Bjerrum length, defined as $l_B \equiv e^2/(4\pi\varepsilon_0\varepsilon k_B T)$ ($\varepsilon_0$ and $\varepsilon$ are vacuum permittivity and the dielectric constant of a solution), is the separation at which the electrostatic interaction between two elementary charges is comparable in magnitude to the thermal energy scale, $k_B T$, (=0.6 kcal mol$^{-1}$ at $T = 298$ K), and is approximately 0.7 nm in water at $T = 298$ K. The Debye length, $\kappa^{-1}$, controls the range of the electrostatic interaction in ionic solutions and is given by $\kappa^{-1} = 1/\sqrt{8\pi l_B N_A I}$, where $N_A$ and $I$ are Avogadro's constant and the ionic strength of the solution, respectively. The electrostatic interaction is calculated for all pairs of charged monomers without cutoff radius. In addition to these interactions, each monomer experiences a hard-core interaction with the rectangular nanochannel, *i.e.*, it is not allowed to approach the channel surface closer than $\sigma/2$.

An additional angle potential ($U_{angle}$) is used to impart the stiffness to the chains. That potential is given by

$$U_{angle}(\theta) = k_{angle}\,(cos\ \theta + 1)^2 \qquad (5)$$

where $\theta$ is the angle between three successive bonds in the DNA molecule and $k_{angle}$ is the force constant of the angle potential. The force constant of the angle potential, $k_{angle}$, is, in fact, the only parameter in our primitive DNA model and was fitted using experimental data in Fig. 2A to give 90 $k_B T$ (=54 kcal mol$^{-1}$).

Using this primitive model, we performed canonical ensemble Monte Carlo (MC) simulations to sample equilibrium configurations of the DNA molecule in a nanochannel. Trial moves included reptation, crank-shaft, continuum configurational bias, and rotation moves.[48–51] Once a single DNA molecule was randomly inserted into the nanochannel, each system was equilibrated until both the system potential energy and the DNA stretch attained a steady-state value. Production runs consisted of a total of $10^9$ MC steps, and were sampled every $10^5$ steps to generate $10^4$ equilibrium configurations. The results given in this study therefore represent averages of at least $10^4$ configurations; the error bars, obtained from block averaging, correspond to one standard deviation from the average. More information about model parameterization and simulation methods can be found elsewhere.[52]

Simulation results are compared with experimental findings and Odijk's theory in Fig. 2. For the case of the DNA stretch in the 250 nm × 250 nm nanochannel (Fig. 2A), the simulation results exhibit good agreement with both experiments and Odijk's theory. Some deviations are seen at low ionic strengths (<0.5 mM). This agreement is expected in that parameter $k_{angle}$ in the primitive model was fitted to these data. For the 250 nm × 400 nm nanochannel (Fig. 2B), our simulation results with a primitive model provide better agreement with experiment than Odijk's theory, which significantly overestimates the DNA stretch at high ionic strengths. However, our simulations do not reproduce the transition behavior near $I = 1.0$ mM that is seen in experiments.

Fig. 2B provides a comparison of the results of simulations with fluorescent images of DNA molecules. Note that simulation snapshots are magnified for better comparison to experiment. As expected, at very low ionic strength ($I = 0.12$ mM), the DNA molecule is extended in the channel direction and exhibits a smooth sinusoidal shape. At $I = 0.62$ mM, it starts to exhibit hairpin-like structures, but the curvature of the loop is still smooth, which indicates that the electrostatic repulsion between monomers persists and prevents sharp turns. Note that the Debye length (about 13 nm) at this ionic strength is slightly longer than the monomer diameter. At higher ionic strengths (>1 mM), the electrostatic repulsion is significantly screened, and the DNA molecule shows several hairpin structures that include sharp turns.

At this point it is important to emphasize some of the limitations of our primitive model. First, it does not consider any specific interaction between monomers or between monomers and the nanochannel other than mean-field type electrostatic interactions and excluded volume interactions (hard-sphere potential). Second, our model does not include explicit water molecules or explicit salt ions. The delicate interplay of multivalent ions in the DNA moiety or the hydrophobic behavior of the DNA molecule in a nanochannel cannot be properly treated in our model. Third, the DNA length in this study is about 10 times shorter than that employed in experiments. It is possible that wavelength modes such as multi-stacking longer than the DNA length in our model may play an important role in the real system. We will present the effect of the DNA length on the structural behavior of DNA in a nanochannel elsewhere.[52]

So far, we have validated Odijk's equation with our experimental observations and our computer simulation results by using two different nanochannels: a square channel 250 nm × 250 nm and a rectangular channel 250 nm × 400 nm. We extended this validation to high aspect ratio channels such as the widths of 600 nm, 800 nm, and 900 nm with the same height of 250 nm (Fig. 3). We used a fixed ionic strength of 0.32 mM (0.2 mM NaCl added to 1/40× TE). The reason to choose this ionic strength is that 0.32 mM is low enough to generate highly stretched DNA molecules in a relatively wide nanochannel, but the ionic strength should be stable or less susceptible to pH change due to the major component of NaCl. Given the same ionic strength, the DNA stretch decreases with increasing channel widths as shown in Fig. 3, which also presents a comparison among our experiment, our simulation and Odijk's theory. Interestingly, the primitive model gives an excellent agreement with experiments in wider channels (>400 nm), which is even better than Odijk theory. This implies that although it has been quite successful in describing the structure of polymers including DNA in a nanochannel, Odijk theory still has room for more sophistication such as considering more structural motifs in addition to hairpins.

Also, Odijk's theory with the OSF equation has a critical shortcoming in applying to biological experiments since OSF equation does not work with multivalent ions.[37,38,53,54] Fig. 4 demonstrates an example of the effect of $Mg^{2+}$ ions, which dramatically reduce DNA's persistence length resulting in shorter stretches in nanochannels compared with $Na^+$ ions. The previous other studies have reported that the addition of multivalent cation reduces not only the electrostatic persistence length ($P_e$) but also the intrinsic non-electrostatic persistence length ($P_0$) (*e.g.* $P_0$ from 50 nm to 25 nm).[37,53] Although the understanding of DNA's persistence length with multivalent ions is known as a very challenging theoretical topic,[53,54] the development of more sophisticated theories is essentially necessary to understand and predict nanochannel confined DNA stretching in complex ionic environments most biological buffers usually have.

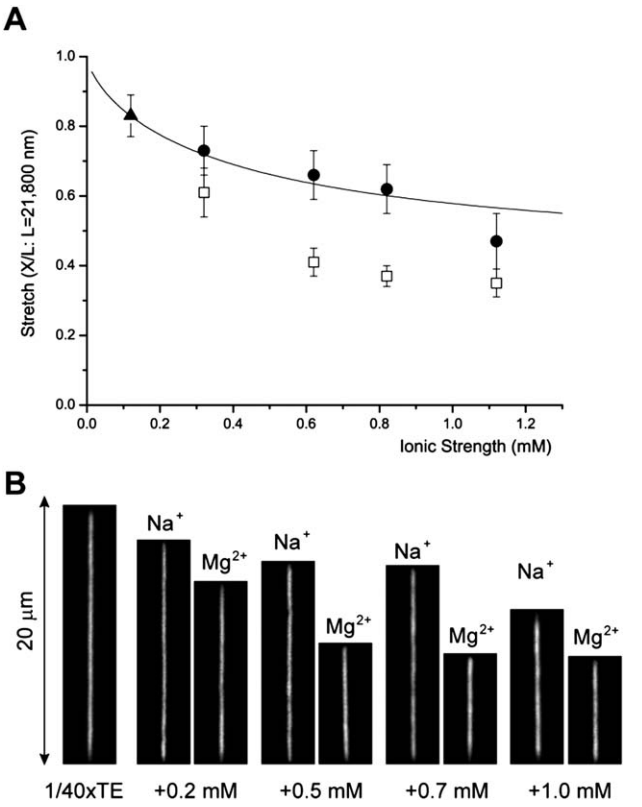


**Fig. 4** Divalent ion effect on DNA stretches in 250 nm × 400 nm channels. (A) The graph shows four points of $MgCl_2$ (□: open square) of equivalent ionic strength of NaCl (●: closed circle) and a reference point of 1/40× TE (▲: filled triangle); these five points are already shown in Fig. 2B. The graph (solid line) of Odijk's equation (eqn (1)) uses 50 nm as $P_0$. Each experimental data point represents measurement from 30 to 80 molecules; error bars show standard deviations of measured lengths. The molecular length is determined by intensity profile analysis as illustrated in Fig. 1. (B) Representative fluorescence images of DNA molecules at the same ionic strength for visual comparison between the effects of monovalent sodium ions and divalent magnesium ions on DNA stretches.

## Experimental

### Fabrication

Here we utilized PDMS nanochannels fabricated by replica molding on silicon wafer mold. Fabrication steps of the silicon wafer mold include interference lithography (IL), lift-off, reactive ion etching, and microchannel overlay. First, the wafer was cleaned in a 1 : 1 mixture of hydrochloric acid and hydrogen peroxide with consecutive sonication in acetone, isopropyl alcohol and deionized water for ten minutes each, and then dried with nitrogen gas. HMDS (Hexamethyldisilane, Fluka) was spin-coated on the substrate to improve the adhesion of photoresist. A negative photoresist (AZ nLOF 2020, Clariant) was diluted with a thinner (AZ1512, Clariant) and spin-coated on the silicon substrate with 150 nm thickness. Interference lithography with a light source of He–Cd laser at 325 nm was used to make a periodic structure. One-beam, some portion of the light, irradiated the photoresist directly, and the other beam projected to the substrate after being reflected from the Lloyd mirror. These two beams projected to the photoresist with a certain angle interfered together and resulted in a sinusoidal exposure. The spatial period can be modulated by changing the incident angle, wavelength of a laser source and developing time. After exposure and the following post-exposure bake, the substrate was dipped into

 

a MIF 500 developer solution for 2 min at room temperature. After these IL processes, 15 nm thick chromium (Cr) layer was deposited on the patterned photoresist and the subsequent lift-off process was performed to define Cr mask for the following etching process with an EKC-830 (Dupont Electronic Technologies) for 30 min at 80 °C. To generate 100, 150, and 250 nm relief patterns, reactive ion etching (RIE) with a gas mixture of $CHF_3$ and $O_2$ was used at a power of 100 W and 5 mTorr and finally the Cr mask was removed with Cr etchant (CR-7, Cyantek).

After fabrication of the nanochannel template, we followed the procedure as described previously.[10] Briefly, a microchannel (5 μm high, 100 μm wide) pattern was overlaid on the nanopatterned wafer using the negative photoresist SU-8 2005 for convenient loading of DNA into nanochannels. A monolayer of tridecafluoro-1,1,2,2-tetrahydro octyl trichloro silane was deposited on the surface of the silicon master mold to promote PDMS releasing in the following replica molding step. The 10 : 1 mixture of PDMS monomer and curing agent was poured onto the patterned silicon wafer master and allowed to cure at 65 °C for 4 h or longer. PDMS devices were treated in an air plasma generator for 30 s (Femto Science Cute Basic) to make the surface hydrophilic. These plasma-treated PDMS devices were stored in high-purity water for 24 hours because PDMS surfaces are reactive immediately following plasma treatment. Afterward, the PDMS devices were washed with 30 mL of 0.5 M EDTA (pH 8.0) for 15 minutes with sonication, then washed with high-purity water by sonicating three times for 15 minutes each and stored in high-purity water before use. Finally, a PDMS device was mounted on a glass previously cleaned in the piranha solution. The DNA samples were loaded into the microchannels *via* capillary action and then lead into the nanochannels by using an applied electrical field (30–50 V across 25 mm) with platinum electrodes inserted into the reservoirs. DNA samples used in this paper have 0.125 μg $\mu L^{-1}$ λ DNA in 0.25 mM Tris and 25 μM EDTA with various NaCl concentrations from 0 mM to 2 mM.

### Imaging

Instead of using anti-bleaching agents, in this study we adjusted the power of a solid-state laser (Coherent Sapphire 488) with an additional optical density filter (NDQ-100-1.00, Korea Electro Optics). The optimum light intensity we used was 0.12 mW measured with a 63× objective lens in a microscope (Zeiss Observer A1). In addition, we removed an emission filter to enhance transmittance of fluorescent light to CCD camera (Roper Scientific CoolSNAP EZ). Instead, a holographic notch filter was used to filter out 488 nm laser source light. Using this microscopic set-up without anti-bleaching agent, we were able to watch and take images of DNA without significant photo-damage such as photolysis or severe photo-bleaching as shown in Fig. 1B. Here we determined the molecular length by the distance between two points where the intensity profiles are equal to the half of the unit intensity: the unit intensity represents the expected intensity if a molecule fully stretches, which value is calculated from a molecule's integrated intensity divided by its contour length (*e.g.* 21 800 nm for λ DNA).

## Conclusions

DNA elongation *via* nanoconfinement is informed by new physical insights, which are readily translated into new molecular analysis approaches in the genomic sciences. Accordingly, we have comprehensively addressed both challenges, through the fabrication of nanochannels for effective presentation of well-stretched DNA molecules, while understanding stretching effects mediated by ionic strengths and channel dimensions guided by using Odijk's theory. For a more rigorous understanding, we have also developed a primitive DNA model in a nanochannel and performed Monte Carlo simulations to evaluate our experimental findings as well as to validate Odijk's analytical equation. Here we demonstrate reasonable agreements among experiment, computer simulation, and theory with some limitations. We believe that our systematic analysis will provide a firm basis for the design of nanochannel platforms offering high-resolution and high-throughput DNA analysis.

## Acknowledgements

This work is supported by the National Science Foundation supported Nanoscale Science and Engineering Center (NSEC; USA), National Institutes of Health, Human Genome Research Institute (NHGRI; USA), the National Research Foundation of Korea (NRF) grant funded by the MEST (2010-0015392, 2010-0028226), and the Converging Research Center Program through MEST (2010K001054). G. Y. Jung thanks the Korea Science and Engineering Foundation (KOSEF) grant (no. R15-2008-006-03002-0, CLEA, NCRC) and the Program for Integrated Molecular System at GIST. R. Chang also acknowledges the support of Korea Research Foundation grant funded by the Korea government (MEST, no. 2009-0077005), Korea Institute of Science and Technology Information (KSC-2009-S01-0015), and a research grant of Kwangwoon University in 2011 for this work.

## References

1 C. W. Fuller, L. R. Middendorf, S. A. Benner, G. M. Church, T. Harris, X. H. Huang, S. B. Jovanovich, J. R. Nelson, J. A. Schloss, D. C. Schwartz and D. V. Vezenov, *Nat. Biotechnol.*, 2009, **27**, 1013–1023.

2 M. Margulies, M. Egholm, W. E. Altman, S. Attiya, J. S. Bader, L. A. Bemben, J. Berka, M. S. Braverman, Y. J. Chen, Z. T. Chen, S. B. Dewell, L. Du, J. M. Fierro, X. V. Gomes, B. C. Godwin, W. He, S. Helgesen, C. H. Ho, G. P. Irzyk, S. C. Jando, M. L. I. Alenquer, T. P. Jarvie, K. B. Jirage, J. B. Kim, J. R. Knight, J. R. Lanza, J. H. Leamon, S. M. Lefkowitz, M. Lei, J. Li, K. L. Lohman, H. Lu, V. B. Makhijani, K. E. McDade, M. P. McKenna, E. W. Myers, E. Nickerson, J. R. Nobile, R. Plant, B. P. Puc, M. T. Ronan, G. T. Roth, G. J. Sarkis, J. F. Simons, J. W. Simpson, M. Srinivasan, K. R. Tartaro, A. Tomasz, K. A. Vogt, G. A. Volkmer, S. H. Wang, Y. Wang, M. P. Weiner, P. G. Yu, R. F. Begley and J. M. Rothberg, *Nature*, 2005, **437**, 376–380.

3 D. R. Bentley, S. Balasubramanian, H. P. Swerdlow, G. P. Smith, J. Milton, C. G. Brown, K. P. Hall, D. J. Evers, C. L. Barnes, H. R. Bignell, J. M. Boutell, J. Bryant, R. J. Carter, R. K. Cheetham, A. J. Cox, D. J. Ellis, M. R. Flatbush, N. A. Gormley, S. J. Humphray, L. J. Irving, M. S. Karbelashvili, S. M. Kirk, H. Li, X. H. Liu, K. S. Maisinger, L. J. Murray, B. Obradovic, T. Ost, M. L. Parkinson, M. R. Pratt, I. M. J. Rasolonjatovo, M. T. Reed, R. Rigatti, C. Rodighiero, M. T. Ross, A. Sabot,

S. V. Sankar, A. Scally, G. P. Schroth, M. E. Smith, V. P. Smith, A. Spiridou, P. E. Torrance, S. S. Tzonev, E. H. Vermaas, K. Walter, X. L. Wu, L. Zhang, M. D. Alam, C. Anastasi, I. C. Aniebo, D. M. D. Bailey, I. R. Bancarz, S. Banerjee, S. G. Barbour, P. A. Baybayan, V. A. Benoit, K. F. Benson, C. Bevis, P. J. Black, A. Boodhun, J. S. Brennan, J. A. Bridgham, R. C. Brown, A. A. Brown, D. H. Buermann, A. A. Bundu, J. C. Burrows, N. P. Carter, N. Castillo, M. C. E. Catenazzi, S. Chang, R. N. Cooley, N. R. Crake, O. O. Dada, K. D. Diakoumakos, B. Dominguez-Fernandez, D. J. Earnshaw, U. C. Egbujor, D. W. Elmore, S. S. Etchin, M. R. Ewan, M. Fedurco, L. J. Fraser, K. V. F. Fajardo, W. S. Furey, D. George, K. J. Gietzen, C. P. Goddard, G. S. Golda, P. A. Granieri, D. E. Green, D. L. Gustafson, N. F. Hansen, K. Harnish, C. D. Haudenschild, N. I. Heyer, M. M. Hims, J. T. Ho, A. M. Horgan, K. Hoschler, S. Hurwitz, D. V. Ivanov, M. Q. Johnson, T. James, T. A. H. Jones, G. D. Kang, T. H. Kerelska, A. D. Kersey, I. Khrebtukova, A. P. Kindwall, Z. Kingsbury, P. I. Kokko-Gonzales, A. Kumar, M. A. Laurent, C. T. Lawley, S. E. Lee, X. Lee, A. K. Liao, J. A. Loch, M. Lok, S. J. Luo, R. M. Mammen, J. W. Martin, P. G. McCauley, P. McNitt, P. Mehta, K. W. Moon, J. W. Mullens, T. Newington, Z. M. Ning, B. L. Ng, S. M. Novo, M. J. O'Neill, M. A. Osborne, A. Osnowski, O. Ostadan, L. L. Paraschos, L. Pickering, A. C. Pike, A. C. Pike, D. C. Pinkard, D. P. Pliskin, J. Podhasky, V. J. Quijano, C. Raczy, V. H. Rae, S. R. Rawlings, A. C. Rodriguez, P. M. Roe, J. Rogers, M. C. R. Bacigalupo, N. Romanov, A. Romieu, R. K. Roth, N. J. Rourke, S. T. Ruediger, E. Rusman, R. M. Sanches-Kuiper, M. R. Schenker, J. M. Seoane, R. J. Shaw, M. K. Shiver, S. W. Short, N. L. Sizto, J. P. Sluis, M. A. Smith, J. E. S. Sohna, E. J. Spence, K. Stevens, N. Sutton, L. Szajkowski, C. L. Tregidgo, G. Turcatti, S. vandeVondele, Y. Verhovsky, S. M. Virk, S. Wakelin, G. C. Walcott, J. W. Wang, G. J. Worsley, J. Y. Yan, L. Yau, M. Zuerlein, J. Rogers, J. C. Mullikin, M. E. Hurles, N. J. McCooke, J. S. West, F. L. Oaks, P. L. Lundberg, D. Klenerman, R. Durbin and A. J. Smith, *Nature*, 2008, **456**, 53–59.

4 R. Drmanac, A. B. Sparks, M. J. Callow, A. L. Halpern, N. L. Burns, B. G. Kermani, P. Carnevali, I. Nazarenko, G. B. Nilsen, G. Yeung, F. Dahl, A. Fernandez, B. Staker, K. P. Pant, J. Baccash, A. P. Borcherding, A. Brownley, R. Cedeno, L. Chen, D. Chernikoff, A. Cheung, R. Chirita, B. Curson, J. C. Ebert, C. R. Hacker, R. Hartlage, B. Hauser, S. Huang, Y. Jiang, V. Karpinchyk, M. Koenig, C. Kong, T. Landers, C. Le, J. Liu, C. E. McBride, M. Morenzoni, R. E. Morey, K. Mutch, H. Perazich, K. Perry, B. A. Peters, J. Peterson, C. L. Pethiyagoda, K. Pothuraju, C. Richter, A. M. Rosenbaum, S. Roy, J. Shafto, U. Sharanhovich, K. W. Shannon, C. G. Sheppy, M. Sun, J. V. Thakuria, A. Tran, D. Vu, A. W. Zaranek, X. Wu, S. Drmanac, A. R. Oliphant, W. C. Banyai, B. Martin, D. G. Ballinger, G. M. Church and C. A. Reid, *Science*, 2010, **327**, 78–81.

5 D. C. Schwartz and M. S. Waterman, *J. Comput. Sci. Tech.*, 2010, **25**, 3–9.

6 T. D. Harris, P. R. Buzby, H. Babcock, E. Beer, J. Bowers, I. Braslavsky, M. Causey, J. Colonell, J. Dimeo, J. W. Efcavitch, E. Giladi, J. Gill, J. Healy, M. Jarosz, D. Lapen, K. Moulton, S. R. Quake, K. Steinmann, E. Thayer, A. Tyurina, R. Ward, H. Weiss and Z. Xie, *Science*, 2008, **320**, 106–109.

7 J. Eid, A. Fehr, J. Gray, K. Luong, J. Lyle, G. Otto, P. Peluso, D. Rank, P. Baybayan, B. Bettman, A. Bibillo, K. Bjornson, B. Chaudhuri, F. Christians, R. Cicero, S. Clark, R. Dalal, A. Dewinter, J. Dixon, M. Foquet, A. Gaertner, P. Hardenbol, C. Heiner, K. Hester, D. Holden, G. Kearns, X. X. Kong, R. Kuse, Y. Lacroix, S. Lin, P. Lundquist, C. C. Ma, P. Marks, M. Maxham, D. Murphy, I. Park, T. Pham, M. Phillips, J. Roy, R. Sebra, G. Shen, J. Sorenson, A. Tomaney, K. Travers, M. Trulson, J. Vieceli, J. Wegener, D. Wu, A. Yang, D. Zaccarin, P. Zhao, F. Zhong, J. Korlach and S. Turner, *Science*, 2009, **323**, 133–138.

8 J. Clarke, H. C. Wu, L. Jayasinghe, A. Patel, S. Reid and H. Bayley, *Nat. Nanotechnol.*, 2009, **4**, 265–270.

9 A. Ramanathan, E. J. Huff, C. C. Lamers, K. D. Potamousis, D. K. Forrest and D. C. Schwartz, *Anal. Biochem.*, 2004, **330**, 227–241.

10 K. Jo, D. M. Dhingra, T. Odijk, J. J. de Pablo, M. D. Graham, R. Runnheim, D. Forrest and D. C. Schwartz, *Proc. Natl. Acad. Sci. U. S. A.*, 2007, **104**, 2673–2678.

11 S. Zhou, J. Herschleb and D. C. Schwartz, in *New Methods for DNA Sequencing*, ed. K. R. Mitchelson, Elsevier Scientific Publishers, 2007.

12 A. Ramanathan, L. Pape and D. C. Schwartz, *Anal. Biochem.*, 2005, **337**, 1–11.

13 E. T. Dimalanta, A. Lim, R. Runnheim, C. Lamers, C. Churas, D. K. Forrest, J. J. de Pablo, M. D. Graham, S. N. Coppersmith, S. Goldstein and D. C. Schwartz, *Anal. Chem.*, 2004, **76**, 5293–5301.

14 A. Valouev, L. Li, Y. C. Liu, D. C. Schwartz, Y. Yang, Y. Zhang and M. S. Waterman, in *Research in Computational Molecular Biology, Proceedings*, ed. S. Miyano, J. Mesirov, S. Kasif, S. Istrail, P. Pevzner and M. Waterman, 2005, vol. 3500, pp. 489–504.

15 A. Valouev, L. Li, Y. C. Liu, D. C. Schwartz, Y. Yang, Y. Zhang and M. S. Waterman, *J. Comput. Biol.*, 2006, **13**, 442–462.

16 A. Valouev, D. C. Schwartz, S. Zhou and M. S. Waterman, *Proc. Natl. Acad. Sci. U. S. A.*, 2006, **103**, 15770–15775.

17 S. G. Zhou, F. S. Wei, J. Nguyen, M. Bechner, K. Potamousis, S. Goldstein, L. Pape, M. R. Mehan, C. Churas, S. Pasternak, D. K. Forrest, R. Wise, D. Ware, R. A. Wing, M. S. Waterman, M. Livny and D. C. Schwartz, *PLoS Genet.*, 2009, **5**, e1000711.

18 P. S. Schnable, D. Ware, R. S. Fulton, J. C. Stein, F. S. Wei, S. Pasternak, C. Z. Liang, J. W. Zhang, L. Fulton, T. A. Graves, P. Minx, A. D. Reily, L. Courtney, S. S. Kruchowski, C. Tomlinson, C. Strong, K. Delehaunty, C. Fronick, B. Courtney, S. M. Rock, E. Belter, F. Y. Du, K. Kim, R. M. Abbott, M. Cotton, A. Levy, P. Marchetto, K. Ochoa, S. M. Jackson, B. Gillam, W. Z. Chen, L. Yan, J. Higginbotham, M. Cardenas, J. Waligorski, E. Applebaum, L. Phelps, J. Falcone, K. Kanchi, T. Thane, A. Scimone, N. Thane, J. Henke, T. Wang, J. Ruppert, N. Shah, K. Rotter, J. Hodges, E. Ingenthron, M. Cordes, S. Kohlberg, J. Sgro, B. Delgado, K. Mead, A. Chinwalla, S. Leonard, K. Crouse, K. Collura, D. Kudrna, J. Currie, R. F. He, A. Angelova, S. Rajasekar, T. Mueller, R. Lomeli, G. Scara, A. Ko, K. Delaney, M. Wissotski, G. Lopez, D. Campos, M. Braidotti, E. Ashley, W. Golser, H. Kim, S. Lee, J. K. Lin, Z. Dujmic, W. Kim, J. Talag, A. Zuccolo, C. Fan, A. Sebastian, M. Kramer, L. Spiegel, L. Nascimento, T. Zutavern, B. Miller, C. Ambroise, S. Muller, W. Spooner, A. Narechania, L. Y. Ren, S. Wei, S. Kumari, B. Faga, M. J. Levy, L. McMahan, P. Van Buren, M. W. Vaughn, K. Ying, C. T. Yeh, S. J. Emrich, Y. Jia, A. Kalyanaraman, A. P. Hsia, W. B. Barbazuk, R. S. Baucom, T. P. Brutnell, N. C. Carpita, C. Chaparro, J. M. Chia, J. M. Deragon, J. C. Estill, Y. Fu, J. A. Jeddeloh, Y. J. Han, H. Lee, P. H. Li, D. R. Lisch, S. Z. Liu, Z. J. Liu, D. H. Nagel, M. C. McCann, P. SanMiguel, A. M. Myers, D. Nettleton, J. Nguyen, B. W. Penning, L. Ponnala, K. L. Schneider, D. C. Schwartz, A. Sharma, C. Soderlund, N. M. Springer, Q. Sun, H. Wang, M. Waterman, R. Westerman, T. K. Wolfgruber, L. X. Yang, Y. Yu, L. F. Zhang, S. G. Zhou, Q. Zhu, J. L. Bennetzen, R. K. Dawe, J. M. Jiang, N. Jiang, G. G. Presting, S. R. Wessler, S. Aluru, R. A. Martienssen, S. W. Clifton, W. R. McCombie, R. A. Wing and R. K. Wilson, *Science*, 2009, **326**, 1112–1115.

19 J. M. Kidd, G. M. Cooper, W. F. Donahue, H. S. Hayden, N. Sampas, T. Graves, N. Hansen, B. Teague, C. Alkan, F. Antonacci, E. Haugen, T. Zerr, N. A. Yamada, P. Tsang, T. L. Newman, E. Tuzun, Z. Cheng, H. M. Ebling, N. Tusneem, R. David, W. Gillett, K. A. Phelps, M. Weaver, D. Saranga, A. Brand, W. Tao, E. Gustafson, K. McKernan, L. Chen, M. Malig, J. D. Smith, J. M. Korn, S. A. McCarroll, D. A. Altshuler, D. A. Peiffer, M. Dorschner, J. Stamatoyannopoulos, D. Schwartz, D. A. Nickerson, J. C. Mullikin, R. K. Wilson, L. Bruhn, M. V. Olson, R. Kaul, D. R. Smith and E. E. Eichler, *Nature*, 2008, **453**, 56–64.

20 B. Teague, M. S. Waterman, S. Goldstein, K. Potamousis, S. G. Zhou, S. Reslewic, D. Sarkar, A. Valouev, C. Churas, J. M. Kidd, S. Kohn, R. Runnheim, C. Lamers, D. Forrest, M. A. Newton, E. E. Eichler, M. Kent-First, U. Surti, M. Livny and D. C. Schwartz, *Proc. Natl. Acad. Sci. U. S. A.*, 2010, **107**, 10848–10853.

21 G. E. Ananiev, S. Goldstein, R. Runnheim, D. K. Forrest, S. G. Zhou, K. Potamousis, C. P. Churas, V. Bergendahl, J. A. Thomson and D. C. Schwartz, *BMC Mol. Biol.*, 2008, **9**, 68.

 

22 H. Yu and D. C. Schwartz, *Anal. Biochem.*, 2008, **380**, 111–121.
23 K. Jo, Y. L. Chen, J. J. de Pablo and D. C. Schwartz, *Lab Chip*, 2009, **9**, 2348–2355.
24 H. Cao, Z. N. Yu, J. Wang, J. O. Tegenfeldt, R. H. Austin, E. Chen, W. Wu and S. Y. Chou, *Appl. Phys. Lett.*, 2002, **81**, 174–176.
25 N. Douville, D. Huh and S. Takayama, *Anal. Bioanal. Chem.*, 2008, **391**, 2395–2409.
26 S. K. Das, M. D. Austin, M. C. Akana, P. Deshpande, H. Cao and M. Xiao, *Nucleic Acids Res.*, 2010, **38**, e177.
27 G. M. Whitesides, E. Ostuni, S. Takayama, X. Y. Jiang and D. E. Ingber, *Annu. Rev. Biomed. Eng.*, 2001, **3**, 335–373.
28 W. Reisner, K. J. Morton, R. Riehn, Y. M. Wang, Z. N. Yu, M. Rosen, J. C. Sturm, S. Y. Chou, E. Frey and R. H. Austin, *Phys. Rev. Lett.*, 2005, **94**, 196101.
29 Q. F. Xia, K. J. Morton, R. H. Austin and S. Y. Chou, *Nano Lett.*, 2008, **8**, 3830–3833.
30 H. Cao, J. O. Tegenfeldt, R. H. Austin and S. Y. Chou, *Appl. Phys. Lett.*, 2002, **81**, 3058–3060.
31 C. C. Hsieh, A. Balducci and P. S. Doyle, *Nano Lett.*, 2008, **8**, 1683–1688.
32 T. T. Perkins, D. E. Smith, R. G. Larson and S. Chu, *Science*, 1995, **268**, 83–87.
33 T. Odijk, *Macromolecules*, 1983, **16**, 1340–1344.
34 T. Odijk, *Phys. Rev. E: Stat., Nonlinear, Soft Matter Phys.*, 2008, **77**, 060901.
35 T. Odijk, *J. Polym. Sci., Polym. Phys. Ed.*, 1977, **15**, 477–483.
36 J. Skolnick and M. Fixman, *Macromolecules*, 1977, **10**, 944–948.
37 C. G. Baumann, S. B. Smith, V. A. Bloomfield and C. Bustamante, *Proc. Natl. Acad. Sci. U. S. A.*, 1997, **94**, 6185–6190.
38 F. J. Solis and M. O. de la Cruz, *J. Chem. Phys.*, 2000, **112**, 2030–2035.
39 S. R. Quake, H. Babcock and S. Chu, *Nature*, 1997, **388**, 151–154.
40 A. Sischka, K. Toensing, R. Eckel, S. D. Wilking, N. Sewald, R. Ros and D. Anselmetti, *Biophys. J.*, 2005, **88**, 404–411.
41 C. Zhang, F. Zhang, J. A. van Kan and J. R. C. van der Maarel, *J. Chem. Phys.*, 2008, **128**, 225109.
42 W. Reisner, J. P. Beech, N. B. Larsen, H. Flyvbjerg, A. Kristensen and J. O. Tegenfeldt, *Phys. Rev. Lett.*, 2007, **99**, 058302.
43 M. Krishnan and E. Petrov, *Comment on Nanoconfinement-Enhanced Conformational Response of Single DNA Molecules to Changes in Ionic Environment*, http://arxiv.org/abs/0805.2100.
44 F. Brochard and P. G. de Gennes, *J. Chem. Phys.*, 1977, **67**, 52–56.
45 R. M. Jendrejack, E. T. Dimalanta, D. C. Schwartz, M. D. Graham and J. J. de Pablo, *Phys. Rev. Lett.*, 2003, **91**, 038102.
46 R. M. Jendrejack, D. C. Schwartz, M. D. Graham and J. J. de Pablo, *J. Chem. Phys.*, 2003, **119**, 1165–1173.
47 P. Cifra, Z. Benkova and T. Bleha, *J. Phys. Chem. B*, 2009, **113**, 1843–1851.
48 M. P. Allen and D. J. Tildesley, *Computer Simulation of Liquids*, Oxford University Press, 1989.
49 D. Frenkel and B. Smit, *Understanding Molecular Simulation*, Academic Press, 2001.
50 J. J. de Pablo, Q. L. Yan and F. A. Escobedo, *Annu. Rev. Phys. Chem.*, 1999, **50**, 377–411.
51 J. J. de Pablo, M. Laso and U. W. Suter, *J. Chem. Phys.*, 1992, **96**, 2395–2403.
52 R. Chang, in preparation.
53 A. V. Dobrynin, *Macromolecules*, 2006, **39**, 9519–9527.
54 E. Geissler, A. M. Hecht and F. Horkay, *Phys. Rev. Lett.*, 2007, **99**, 267801.